COSMOLOGY TODAY-MODELS AND CONSTRAINTS*

T. Padmanabhan

Inter-University Centre for Astronomy and Astrophysics
Post Bag 4, Ganeshkhind,
Pune - 411 007, India
email: *paddy@iucaa.ernet.in*

Cosmological models for structure formation are severely constrained by several of the recent observational results. We now have observations which probes the power spectrum of fluctuations from about 0.5 h^{-1} Mpc to 3000 h^{-1}Mpc. These probes and the constraints they imply on models for structure formation are reviewed.

1. Recipe for the Universe

All the popular models for structure formation are based on three key ingredients: (a) a model for the background universe (b) some mechanism for generating small perturbations in that universe and (c) specification of the nature of the dark matter. Let us begin by considering each of these ingredients.

The background universe is usually taken to be a Friedmann model with an expansion factor $a(t)$. Such a model is completely specified if the composition of the energy density and the Hubble constant are specified. We will take $H_0 = 100h$ kms^{-1} Mpc^{-1}(or $H_0^{-1} = 3000h^{-1}$ Mpc in units with $c = 1$) and express the energy density of the various species in terms of the critical density $\rho_c = (3H_0^2/8\pi G) = 1.88h^2 \times 10^{-29}gcm^{-3} = 6.94 \times 10^{10}h_{50}^2 M_\odot$Mpc^{-3}, by writing $\rho_i = \Omega_i \rho_c$ for the i^{th} species. From various observations[1], we can impose the following constraints: (i) $0.011h^{-2} \lesssim \Omega_B \lesssim 0.016h^{-2}$ (ii) $\Omega_{\rm vac} \lesssim 0.8$ (iii) $\Omega_{\rm lum} \simeq 0.007h$ (iv) $\Omega_R = 4.85h^{-2} \times 10^{-5}$ (v) $\Omega_{\rm total} \equiv \Omega \gtrsim 0.3$. Theoretical models strongly favour $\Omega = 1$ and it is usual to invoke either a cosmological constant and/or nonbaryonic dark matter to achieve this. We shall denote by Ω_{DM} the total contribution due to all nonbaryonic energy densities.

Given these parameters one can construct a background Friedmann model. As an example, consider a model with $\Omega_{DM} \gg \Omega_B$ (say, $\Omega_{DM} \simeq 0.9$, $\Omega_B \simeq 0.1$), $\Omega_{vac} = 0$ and $\Omega_R = \Omega_\gamma$. The evolution of such a model will proceed along the following lines: During the very early phases of the evolution, the universe will be radiation-dominated with $a(t) \propto t^{1/2}$. A transition to matter dominated phase will occur at the redshift of $z \simeq z_{eq}$ where $(1 + z_{eq}) = (\Omega_{DM}/\Omega_R) \simeq 3.9 \times 10^4 \Omega h^2$. [For $t > t_{eq}$, the form of $a(t)$ depends on the value of Ω. If $\Omega = 1$, then $a(t) \propto t^{2/3}$; this is a good approximation for $z \gtrsim 100$ in all models]. The baryons and the electrons will be strongly coupled to the photons at this epoch. Somewhat later in the evolution, at $z \simeq z_D$ with $z_D \simeq 1100$, the electrons and positive ions will combine together to form neutral atoms of Hydrogen and Helium. The photons will decouple from matter at this epoch and will propagate thereafter with negligible scattering. The structures like galaxies etc., will form significantly later at $z \ll z_D$.

The evolution can be different if Ω_{vac} is significant. As a second example, consider a universe with $h = 0.7$, $\Omega = 1$, $\Omega_B = 0.03$, $\Omega_{DM} = 0.17$ and $\Omega_{vac} = 0.8$. In such a model, $(\rho_{DM}/\rho_{vac}) = 0.25\ (1 + z)^3$ so that for $z \lesssim z_{vac} \simeq 0.59$ the vacuum energy ('cosmological constnt') dominates over

* To appear in the proceedings of the **VI - IAU Asian Pacific Regional Meeting on Astronomy,** Eds., N. Dadhich and V. Kapahi, (Indian Academy of Sciences Publications, 1994).
IUCAA - 27/93

matter. For $z \ll z_{eq} \simeq 2300$, the expansion factor will evolve as $a(t) = (\Omega_{DM}/\Omega_{vac})^{1/3} \sinh^{2/3}(3\sqrt{\Omega_{vac}}\, H_0 t/2)$. The 'age' of such a universe will be larger than a model with $\Omega = 1$, $\Omega_{vac} = 0$ at all redshifts. [For example, $t_0 = 1.1 H_0^{-1}$ for this model compared to $0.667 H_0^{-1}$ for the $\Omega_{vac} = 0$ model.]. As we shall see, such models can sometimes help to overcome the difficulties in more conventional models.

Models for structure formation assume that small perturbations in the energy density existed at very early epochs. These perturbations can then grow via gravitational instability leading to the structures we see today. In most of the models these perturbations are generated by processes which are supposed to have taken place in the *very* early universe (say, at $z \gtrsim 10^{18}$). Inflationary models – which are probably the most successful ones[2] in this regard – produce density perturbations with an initial power spectrum $P_{\rm in}(k) \simeq Ak$. Since each logarithmic interval in k space will contribute to the energy density an amount $\Delta_\rho^2(k) \equiv d\sigma^2/d(lnk) = (k^3 P(k)/2\pi^2)$ we find that $\Delta_\rho^2 \propto k^4$ for $P \propto k$. The contribution to gravitational potential from the same range will be $\Delta_\varphi^2 = \Delta_\rho^2(9H_0^4/4k^4a^2)$ which is independent of k if $\Delta_\rho^2 \propto k^4$. Such a "scale-invariant" spectrum is produced in some other seeded models as well. All these models need to be fine-tuned to keep the amplitude of the fluctuations small upto, say, $z \gtrsim 10^3$.

Given a Friedmann model with small inhomogeneities described by a power spectrum $P(k, z_{\rm in})$ at a high redshift $z = z_{\rm in}$, we can predict unambigiously the power spectrum $P(k, z_D)$ at $z \approx z_D \approx 10^3$, since we can use linear perturbation theory during this epoch. The shape of the spectrum at $z = z_D$ will not be a pure powerlaw because the gravitational amplifiction is wavelength-dependent. In general, the power at small scales is suppressed (relative to that at large scales) due to various physical processes, and, the exact shape at $z = z_{\rm D}$ depends on the kind of dark matter present in the universe. In a universe dominated by "hot dark matter" particles of mass $m \simeq 30eV$, the power per logarithmic interval in $k-$space, $\Delta(k) = (k^3 P(k)/2\pi^2)^{1/2}$, is peaked at $k = k_{\rm max} \equiv 0.69 k_{FS} \equiv 0.11$ Mpc$^{-1}(m/30eV)$ and falls exponentially for $k > k_{\rm max}$. Hence, in these models, the scale $k = k_{\rm max}$ will go nonlinear first and smaller structures have to form by fragmentation. If the universe is dominated by "cold dark matter" particles with mass $m \gtrsim 35$GeV, then $\Delta(k)$ is a gently increasing function of k for small k. If we set $P(k) \propto k^n$ locally, the index n changes from 1 at $k^{-1} \gtrsim 200h^{-1}$Mpc to 0 at $k^{-1} \simeq 10h^{-1}$Mpc and in about (-2) at $k^{-1} \simeq 1h^{-1}$ Mpc. In such models small scales will go nonlinear first and the structure will develop heirarchically[3].

The situation is more complicated if two different kinds of dark matter is present or if the cosmological constant is nonzero. The presence of the cosmological constant adds to the power at large scales but suppresses the growth of perturbations at small scales. Similar effect takes place if a small fraction of the dark matter is hot and the bulk of it is cold (eg. $\Omega_{\rm HDM} \simeq 0.2$, $\Omega_{CDM} \simeq 0.8$). In both the cases there will be more power at large scales and less power at small scales, compared to standard CDM model. The spectrum $\Delta(k)$ is still a gently increasing function of k and small scales go nonlinear first.

The fact, that one can compute the power spectrum at $z \simeq z_D$ analytically, allows one to predict large scale anisotropies in CMBR unambiguously in any given model. Comparing this prediction with the anisotropy observed by COBE one can fix the amplitude A of the power spectrum. For a wide class[4] of the models, $\Delta(k) \cong 10^{-3}(kL)^2$ with $L \simeq (24 \pm 4)h^{-1}$ Mpc for $k^{-1} \gtrsim 80h^{-1}$ Mpc. For CDM like models the function $\Delta(k)$ flattens out at larger k and is about unity around $k^{-1} \simeq 8h^{-1}$ Mpc. In pure HDM models, $\Delta(k)$ has a maximum value of $\Delta_m \simeq 0.42h^{-2}(m/30eV)^2$ at $k_m \simeq 0.11$Mpc$^{-1}(m/30eV)$ and decreases exponentially at $k \gtrsim k_m$.

The evolution of the power spectrum after decoupling (for $z < z_{\rm D}$) is more difficult to work out theoretically. In general, the power spectrum grows in amplitude (preserving the shape), as long as the perturbations are small[3]. In this case, we can write $\Delta(k, z) = [f(z)/f(z_D)]\,\Delta(k, z_D)$ for $z < z_D$. For example, in CDM models with $\Omega = 1, f(z) = (1+z)^{-1}$; thus $\Delta(k)$ grows by a factor 10^3 at all scales between the epoch of decoupling ($z_D \simeq 10^3$) and the present epoch ($z = 0$), if we assume that linear theory is valid at all scales. The resulting $\Delta_0(k)$, obtained by linear extrapolation, is often used to specify the properties of the models. This spectrum correctly describes the power at large scales (say, $k^{-1} \gtrsim 30h^{-1}$ Mpc) where $\Delta_0 \lesssim 0.1$. Figure 1 shows the density contrast $\sigma(R)$ computed from the linearly extrapolated power spectrum $\Delta_0(k)$ in four diffrent models. The density

contrast $\sigma(R)$ measures the rms fluctuations in mass within a randomly placed sphere of radius R; upto factors of order unity, $\sigma(R) \simeq \Delta(k \simeq R^{-1})$.

At small scales, the true power $\Delta_{\rm true}(k)$ will be larger than $\Delta_0(k)$ due to nonlinear effects. There has been several attempts in the literature to understand the form of $\Delta_{\rm true}(k)$ at $k^{-1} \lesssim 30h^{-1}$ Mpc. Since dark matter particles interacts only through gravity, it is possible to study the formation of dark matter structures by numerical simulations. Figure 2 shows the actual nonlinear evolution of the power spectrum with redshift based on numerical simulations. For a wide class of models, one can relate[5] the nonlinear and linear density contrasts by a set of power laws of the form: $\sigma^2_{NL}(a,x) = A[\sigma^2_L(a,l)]^n$ with $l^3 = x^3(1+\sigma^2_{NL})$ where $A = n = 1$ for $\sigma^2_L \leq 1.2; A = 0.794, n = 2.9$ for $1.2 \leq \sigma^2_L \leq 6.0$ and $A = 9.12, n = 1.55$ for $\sigma^2_L \geq 6.0$. This relation shows that σ_{NL} is steeper than σ_L.

In fact, for $k^{-1} \gtrsim 2h^{-1}$ Mpc, one can even neglect the evolution of the gravitational potential and study the motion of the particles in a potential 'frozen' in time. Such an approximation reproduces[6] the results of exact N-body simulations quite accurately for $k^{-1} \gtrsim 1h^{-1}$ Mpc. Figure 3 shows the results of such a simulation. We see that the central effect in cosmological clustering is the motion of particles towards the minimum of the initial potential field.

At still smaller scales, the evolution is complicated by two effects. Firstly, the minima of gravitational potential changes significantly both in depth and location at small scales, requiring a full N-body simulation to understand the dark matter dynamics. Secondly, it is important to understand gas dynamical processes before one can compare theory and observations at small scales. Since baryons can dissipate energy and sink to the minima of the dark matter potential wells, the statistical properties of visible galaxies and dark matter halos could be quite different. The situation is further complicated by the fact that in hierarchical models, considerable amount of merging takes place at small scales. It is usual to quantify our ignorance at these scales by a 'bias' (acronym for 'Basic Ignorance of Astrophysical Scenarios') factor b and write $\xi_{\rm gal}(r) = b^2\xi_{\rm mass}(r)$. Such a parametrisation is useful if b is idependent of scale and morphology of galaxies. This seems to be somewhat unlikely. Since small scale observations are based on galactic properties, while theoretical calculations usually deal with underlying mass distribution, any scale (or morphology) dependence of b could play havoc with predictive power of the theory.

It is clear from the above discussions that our theoretical understanding is best at large scales ($k^{-1} \gtrsim 30h^{-1}$ Mpc) where linear theory is valid, $\Delta_0(k)$ is well determined and baryonic astrophysical processes are not important. At the intermediate scales ($3h^{-1}$ Mpc$\lesssim k^{-1} \lesssim 30h^{-1}$ Mpc), it is not too difficult to understand the dark matter dynamics by some approximation but the baryonic physics begins to be nontrivial. At still smaller scales, ($k^{-1} \lesssim 3h^{-1}$ Mpc) there is considerable uncertainty in our theoretical predictions. We shall now turn to the observational probes of the power spectrum at different scales.

2. Probing the power spectrum

One of the direct ways of constraining the models is to estimate the density contrast $\sigma_{\rm obs}(R)$ from observations at different scales and compare it with the theoretically predicted values. Fortunately, we now have observational probes covering four decades of scales from 10^{-1} Mpc to 10^3 Mpc. We shall discuss the probes of different scales in the decreasing order.

(a) Near horizon scales: $(300 - 3000)h^{-1}$Mpc

COBE DMR: These scales are so large that the best way to probe them is by studying the MBR anisotropy at angular scales which correspond to these linear scales. Since a scale L subtends an angle $\theta(L) \cong 1^\circ(L/100h^{-1}$ Mpc) at $z \simeq z_D$, the $(\Delta T/T)$ observations at $(3^\circ - 30^\circ)$ probe these scales. The COBE-DMR observations[7] of $(\Delta T/T)_{\rm rms}$ and $(\Delta T/T)_Q$ allow one to obtain the following conclusions: (i) $\sigma(10^3h^{-1}$ Mpc$) \simeq 5 \times 10^{-4}$ (ii) The power spectrum at large scales is $P_{\rm in}(k) \simeq Ak^n$ with $n \cong 1.1 \pm 0.6$ and, if we take $\Omega = 1, n = 1$, then $A^{1/4} \cong (24 \pm 4)h^{-1}$ Mpc (iii) In this[4] range, $\sigma(R) \cong (24 \pm 4h^{-1}$ Mpc$/R)^2$.

Primordial gravity waves: A large class of inflationary models also predict the existence of a stochastic background of gravitational waves which can be used to probe scales $L \simeq H_0^{-1} \simeq 3000h^{-1}$ Mpc. The expected energy density of these waves is about $\Omega_g \simeq 3 \times 10^{-9}$, and the spectrum is scale-invariant[8]. Unfortunately, the current generation of gravity wave detectors cannot observe this background.

(b) Very large scales : $(80 - 300)h^{-1}$ Mpc

CMBR probes: These scales span $(0.8° - 3°)$ in the sky at $z \simeq z_D$. Several ground based and balloon-borne experiments to detect anisotropy in MBR probe this scale. For example, the UCSB South Pole experiment has recently reported[9] a preliminary 'detection' of $(\Delta T/T) \simeq 10^{-5}$ at 1.5° scale, and a 95% confidence level bound of $(\Delta T/T) < 5 \times 10^{-5}$. This translates into the constraint of $\sigma(10^2 h^{-1}\ \text{Mpc}) \lesssim 5 \times 10^{-2}$.

CfA2 survey: Some galaxy surveys, notably CfA2 survey and pencil-beam surveys probe scales which are about $10^2 h^{-1}$ Mpc in depth[10]. Unfortunately, the statistics at these large scales is not good enough for one to obtain $\sigma(R)$ directly from these surveys.

(c) Large scales : (40 - 80) h^{-1} Mpc

CMBR probes: The scales correspond to $\theta_{MBR} \simeq (24' - 48')$ and are probed by the experiments looking for small angle anisotropies in MBR. The claimed detection[11] by MIT-MASM of $(\Delta T/T) \cong (0.5 - 1.9) \times 10^{-5}$ at $\theta \simeq 28'$, if confirmed, will give a bound of $\sigma(50h^{-1}\ \text{Mpc}) \lesssim 0.3$.

Galaxy Surveys: Several galaxy surveys, in particular the IRAS-QDOT and APM surveys, give valuable information about this range[12]. The angular correlation of galaxies, measured by APM survey is $\omega(\theta) \simeq (1 - 5) \times 10^{-3}$ at $\theta \simeq 14°$. This corresponds to $\sigma(50h^{-1}\ \text{Mpc}) \cong 0.2$. What is more important, these surveys give valuable information about the shape of the power spectrum in this range.

Large scale velocity field: Using distance indicators which are independent of Hubble constant, it is possible to determine the peculiar velocity field $v(R)$ of galaxies upto about $80h^{-1}$ Mpc or so. The motion of these galaxies can be used to map the underlying gravitational potential at these scales. Careful analysis of observational data shows[13] that $v(40h^{-1}\ \text{Mpc}) \simeq (388 \pm 67)\ \text{kms}^{-1}$ and $v(60h^{-1}\ \text{Mpc}) \simeq (327 \pm 82)\ \text{kms}^{-1}$. From these values it is possible to deduce that $\sigma(50h^{-1}\ \text{Mpc}) \simeq 0.2$. These observations also allow us to determine the value of the parameter $(\Omega^{0.6}/b_{\text{IRAS}})$ where b_{IRAS} is the bias factor with respect to IRAS galaxies. One finds that $(\Omega^{0.6}/b_{\text{IRAS}}) = 1.28^{+0.75}_{-0.59}$ which implies that if $\Omega = 1$, then $b_{\text{IRAS}} = 0.78^{+0.66}_{-0.29}$ and if $b_{\text{IRAS}} = 1$ then $\Omega = 1.51^{+1.74}_{-0.97}$.

Clusters and voids: The cluster-cluster corelation function and the spectrum of voids in the universe can, in principle, tell us something about these scales. Unfortunately, the observational uncertainties are so large that one cannot yet make quantitative predictions.

These scales are probably most valuable in constraining the shape of the power spectrum, which will be beginning to deviate from the primordial form at these scales. It should be noted that a straight extrapolation of COBE-DMR result $\sigma(R) \cong (24h^{-1}\text{Mpc}/R)^2$ to $R = 50h^{-1}$ Mpc gives $\sigma_{\text{COBE}}(50h^{-1}\ \text{Mpc}) \simeq 0.2$. This is consistent with the result from large scale streaming $\sigma_{\text{LSV}}(50h^{-1}\text{Mpc}) \simeq 0.2$, which is not surprising since both probe the gravitational potential of dark matter. However, the result of galaxy surveys –based on *visible* matter –also gives $\sigma_{\text{APM}}(50h^{-1}\ \text{Mpc}) \simeq 0.2$. This suggests that observations are *consistent* with the conclusion that biasing is unimportant at $R \simeq 50h^{-1}$ Mpc.

(d) Intermediate scales : $(8 - 40)h^{-1}$ Mpc

These scales span the angular scales of $\theta_{\text{MBR}} \simeq (4.8' - 24')$ and contains a background mass of $M_{\text{smooth}} \simeq (1.2 \times 10^{15} - 1.5 \times 10^{17})\Omega h_{50}^{-1} M_\odot$. Note that the finite duration of the recombination epoch ($\Delta z \simeq 80$) wipes out anisotropies at angular scales smaller than $\theta_{\text{min}} \simeq 8'\Omega^{1/2}h$. However, it is possible to probe these scales directly.

Galaxy Surveys: The galaxy - galaxy correlation function $\xi_{gg} \cong [r/5.4h^{-1}Mpc]^{-1.8}$ is fairly well determined at these scales. Direct observations suggest that $\sigma_{\text{gal}}(8h^{-1}\ \text{Mpc}) \simeq 1$ but the σ_{DM} and σ_{gal} at these scales can be quite different because of biasing.

Cluster Surveys: There have been several attempts to determine the correlation function of clusters of different classes. It is generally believed that $\xi_{cc} \simeq (r/L)^{-1.8}$ with $L \simeq 25h^{-1}$ Mpc. The index $n = 1.8$ is fairly well determined though the scale L is not; in fact, L seems to depend on the richness class of the cluster. The quantity $(\xi_{cc}/\xi_{gg})^{1/2}$ can be thought of as measure of the relative bias between cluster and galaxy scales. Observations suggest[14] that this quantity depends on the cluster class and varies in the range $(2-8)$. The observational uncertainties are still quite large for this quantity to be of real use; but if the observations improve we will have valuable information from ξ_{cc}.

Abundance of rich clusters: The scale $R = 8h^{-1}$ Mpc contain a mass of $1.2 \times 10^{15}\Omega h_{50}^{-1} M_\odot$. When this scale becomes nonlinear, it will reach an overdensity of about $\delta \simeq 178$, or – equivalently – it will contract to a radius of $R_f \simeq (8h^{-1}$ Mpc$)\ /(178)^{1/3} \simeq 1.5h^{-1}$ Mpc. A mass of $10^{15}M_\odot$ in a radius of 1.5 Mpc is a good representation of Abell clusters we see in the universe. *This implies that the observed abundance of Abell clusters can be directly related to* $\sigma(8h^{-1}$ Mpc). Several people have attempted to do this[15]; the final results vary depending on the modelling of Abell clusters, and gives $\sigma(8h^{-1}$ Mpc$) \simeq (0.5-0.7)$. Since $\sigma_{gal}(8h^{-1}$ Mpc$) \simeq 1$, this shows that $b \simeq (1.23-2)$ at $8h^{-1}$ Mpc.

It is possible to give this argument in a more general context[16]. Suppose that the contribution to critical density from collapsed structures with mass larger than M is $\Omega(M)$, at a given redshift z. Then one can show that

$$\Omega(M) = erfc\left[\frac{\delta_c(Hz)}{\sqrt{2}\sigma_0(M)}\right]$$

where $\delta_c = 1.68$ and erfc(x) is the complementary error function. Figure 4 shows $\Omega(M)$ as a function of $\sigma_0(M)$ for various values of z. The Abell clusters (at $z = 0$) contribute in the range $\Omega \simeq (0.001-0.02)$. Even with such a wide uncertainty, we get $\sigma_{clus} \simeq (0.5-0.7)$.

(e) Small scales : $(0.05-8)h^{-1}$ Mpc

These scales corresponds to structures with $M_{smooth} \simeq (3 \times 10^8 - 1.2 \times 10^{15})\ \Omega h_{50}^{-1} M_\odot$ and we have considerable amount of observational data covering these scales. Unfortunately, it is not easy to make theoretical predictions at these scales because of nonlinear, gas dynamical, effects.

Epoch of galaxy formation: Observations indicate that galaxy like structures have existed even at $z \simeq 3$. This suggests that there must have been sufficient power at small scales to initiate galaxy formation at these high redshifts. Unfortunately, we do not have reliable estimate for the abundance of these objects at these redshifts and hence we cannot directly use it to constrain $\sigma(R)$.

Abundance of quasars: The luminosity function of quasars is fairly well determined upto $z \approx 4$. If the astrophysical processes leading to quasar formation are known, then the luminosity function can be used to estimate the abundance of host objects at these redshifts. Though these processes are somewhat uncertain, most of the models for quasar formation suggest[16] that we must have $\sigma(0.5h^{-1}$ Mpc$) \gtrsim 3$.

Absorption systems: The universe at $1 \lesssim z \lesssim 5$ is also probed by the absorption of quasar light by intervening objects. These observations suggest that there exist significant amount of clumped material in the universe at these redshifts with neutral hydrogen column densities of $N_{HI} \simeq (10^{15} - 10^{22})\mathrm{cm}^{-2}$. We can convert these numbers into abundances of dark matter halos by making some assumptions about this structure. We find that[17] in the redshift range of $z \simeq (1.7-3.5)$ damped Lyman alpha systems contribute a fractional density of $\Omega_{LY} \simeq (0.06-0.23)$. This would require $\sigma(10^{12}M_\odot) \simeq (3-4.5)$. This is also shown in figure 4.

Gunn-Peterson bound: While we do see absorption due to *clumped* neutral hydrogen, quasar spectra do not show any absorption due to smoothly distributed neutral hydrogen. Since the universe became neutral at $z \lesssim z_D \simeq 10^3$, and since galaxy formation could not have made all the neutral hydrogen into clumps, we expect the IGM to have been ionised sometime during $5 \lesssim z \lesssim 10^3$. It is not clear what is the source for these ionising photons. Several possible scenarios (quasars, massive primordial stars, decaying particles etc.) have been suggested in the literature though none of these appears to be completely satisfactory[18]. In all these scenarios, it is necessary to form structures as $z \gtrsim 5$ so that an ionising flux of about $J = 10^{-21}$ergs cm^{-2}s^{-1} Hz^{-1} sr^{-1} can be generated at these epochs.

Once again, it is difficult to convert this constraint into a firm bound on σ though it seems that $\sigma(0.5h^{-1}\ \mathrm{Mpc}) \gtrsim 3$ will be necessary.

Direct observation 21 cm line: It will be possible to observe the neutral hydrogen at $z \gtrsim 3$ by observing the redshifted 21 cm line. The searches performed so far have not led to reliable detections. In a standard CDM model one would expect fluxes of (1.5 - 3) mJy from protocondensates with abundances of $N \simeq (10^{-8} - 10^{-7})\ \mathrm{Mpc}^{-3}$ at $z = 3.3$. These fluxes should be detectable[19] in the near future with GMRT.

The constraints discussed in this section are summarised in figure 5.

3. Scorecard for the models

The simplest models one can construct will contain a single component of dark matter, either cold or hot. Such models are ruled out by the observations. The HDM models, normalised to COBE result will have maximum power of $\triangle_m \cong 0.42h^{-2}(m/30eV)^2$ at $k = k_m = 0.11\ \mathrm{Mpc}^{-1}(m/30eV)$. In such a case, structures could have started forming only around $(1 + z_c) \cong (\triangle_m/1.68) \cong h_{50}^{-2}(m/30eV)^2$ or at $z_c \cong 0$. We cannot explain a host of high-z phenomena with these models. The pure CDM models face a different difficulty. These models, normalised to COBE, predict $\sigma_8 \simeq 1$, which is too high. When nonlinear effects are taken into account, one obtains $\xi_{gg} \propto r^{-2.2}$ for $h = 0.5$ which is too steep compared to the observed value of $\xi_{gg} \propto r^{-1.8}$. In other words, CDM models has wrong shape to account for the observations.

The comparison of CDM spectrum with observations suggests that we need more power at large scales and less power at small scales. This is precisely what happens in models with both hot and cold dark matter or in models with nonzero cosmological constant. These models have been extensively studied during the last year, and they fare well as far as large and intermediate scale observations are concerned. However, they have considerably less power at small scales compared to CDM model. As a result, they do face some difficulty[17] in explaining the existence of high redshift objects like quasars. For example[20], a model with 30% HDM and 70% CDM will have $\sigma_{0.5} \simeq 1.5$; to explain the abudnance of quasars comfortably one needs $\sigma_{0.5} \simeq 3.0$. If we use a more liberal criterion of $\sigma(10^{11}M_\odot) \gtrsim 2$ [which corresponds to $\sigma_{0.4} \gtrsim 2$ for $h = 0.5$] then one is left with a very narrow window in the $(\Omega_\nu - h)$ plane which accounts for all observations. Demanding that $\sigma(10^{12}M_\odot) > 2$ [which is equivalent to saying that $10^{12}M_\odot$ objects must have collapsed at a redshift of $z_{12} = (2/1.68) - 1 \simeq 0.2$] will completely rule out this model.

Similar difficulties exist[21] in models with cosmological constant. On demanding that: (i) the age of the universe is between (13-15)Gyr; (ii) the galaxy survey results are reproduced; (iii) σ_8 is at an acceptable range and (iv) the large scale streaming motions are correctly reproduced, one finds that no acceptable window exists in the $(\Omega_{\mathrm{CDM}} - h)$ plane for a model with $\Omega_{\mathrm{CDM}} + \Omega_\Lambda = 1$. If the constraint (iv) is relaxed to a 2σ level then a narrow window exists in this plane.

The comparison of models show that it is not easy to accommodate all the observtions even by invoking two components to the energy density. (These models also suffer from serious problems of fine-tuning). By and large, the half-life of such quick-fix models seem to be about 2-3 years. One is forced to conclude that to make significant progress it is probably necessary to perform a careful, unprejudiced analysis of: (a) large scale observational results and possible sources of error and (b) small scale astrophysical processes.

Acknowledgements

I thank J.S. Bagla, O. Lahav, M. Rees, K. Subramanian and S.D.M. White for useful discussions.

REFERENCES

1. See for e.g., Carney, B.W. and Latham, D.W., in *Dark Matter in the Universe* (eds. Kormendy, J. and Knapp, G.R.), IAU Symposium 117, Reidel, Dordrecht, 1987, p.39; Tremaine, S. and Lee, H.M., in *Dark Matter in the Universe*, World Scientific, Singapore, 1987, p. 103; Rubin, V.C., in *After the First Three Minutes* (eds. Holt, S.S., Bennett, C.L. and Trimble, V.), AIP, New York, 1991. Observational status of the primordial nucleosynthesis is reviewed, for example, Pagel, B.E.J., *Phys. Scr.,* 1991, **T36**, 7.
2. Guth, A. and Pi, S.Y., *Phys. Rev. Lett.,* 1982, 49, 1110; Hawking, S.W., *Phys. Letts.,* 1982, **B115**, 295; Starobinsky, A.A., *Phys. Lett.,* 1982, **B117**, 175; Padmanabhan, T., Seshadri, T.R. and Singh, T.P., *Phys. Rev.,* 1989, **D39**, 2100. For a review, see Narlikar, J.V. and Padmanabhan, T., *Annu. Rev. Astron. Astrophys.,*1991, **29**, 325.
3. For a detailed discussion of these effects, see, e.g., T. Padmanabhan (1993) *Structure formation in the Universe* (Cambridge University Press, UK), chap.4.
4. T. Padmanabhan, D. Narasimha, *MNRAS* (1992) **259**, 41P.
5. J.S. Bagla and T. Padmanabhan (1993) IUCAA preprint; Hamilton, AJS et al; (1991) *Ap. J.*, **374**, L1.
6. J.S. Bagla and T. Padmanabhan (1993) *MNRAS* (in press); J.S. Bagla and T. Padmanabhan (1993) IUCAA preprint 22/93 *(to appear in the proceedings of VI IAU Asian Pacific Regional Meeting on Astronomy,1993).*
7. Smoot, G.F. et al.,*Ap. J.*, (1992) **396**, L1.
8. See eg., Fabbri, R. and Pollock, M.D. (1983) *Phys. Letts B* **125**, 445; Starobinsky, A.A. (1985), *Sov. Astron. Letts*, **9**, 302.
9. Schuster, J. et al. *Ap.J.* (1993) **412**, L47.
10. Broadhurst, T. et al., (1990) Nature **343**, 726; Vogeley, M.S. et al., (1992) *Ap.J. Letts*, **391**, L5.
11. Cheng, E.S. et al., (1993) preprint
12. Rowan-Robinson, M., et al., *MNRAS,* 1990, **247**, 1; Efstathiou, G. et al., *MNRAS,* 1990, **247**, 10p. Saunders, W. et al., *Nature,* 1991, **349**, 32.
13. Bertschinger, E. and Dekel, A., *Ap. J.,* 1989, **336**, L5; Dekel, A., Bertschinger, E. and Faber, S.M., *Ap. J.,* 1990, **364**, 349; Bertschinger, E. et al.,*Ap. J.,* 1990, **364**, 370.
14. Dalton, G.D. et al., (1992) *Ap.J. Letts* **390**, L1; Nicol, R.C. et al., (1992) *MNRAS* **255**. 21p; Bahcall, N. and West, M. (1992) *Ap. J.* **270**, 70; Postman, M. et al., (1992) *Ap. J.*, **384**, 404.
15. See eg., White, S.D.M. et al., *MNRAS,*(1993) **262**, 1023.
16. See eg., Hachnelt, M.G. (1993) IOA preprint.
17. K. Subramanian, T. Padmanabhan (1993) preprint.
18. Gunn, J.E. and Peterson, B.A., *Ap. J.,* 1965, **142**, 1633; Steidel, C.C. and Sargeant, W.L.W., *Ap. J. Letts.,* 1987, **318**, L11; Also see Schneider et al., *Astron. J.,* 1989, **98**, 1951. See eg. Shapiro, P.R. and Giroux, M.L., *Ap. J. Letts.,* 1987, **321**, L107; Couchman, H.P. M. and Rees, M.J., *MNRAS,* 1986, **221**, 1513. Miralda-Esundé, J. and Ostriker, J.P., *Ap. J,* (1990), **350** , 1.
19. K. Subramanian, T. Padmanabhan (1993) *MNRAS*, in press.
20. Pogosyan, D. Yu and Starobinsky, A.A. (1993) IOA preprint.
21. Kofman, L et al., (1993) CITA preprint.

Figure Captions

Fig. 1: The linearly extrapolated density contrast, filtered by a sphere of radius R, in four different models. All models are for $\Omega_t = 1$, and normalised by COBE. Solid line: CDM model; Dashed

line Λ+ CDM model with $\Omega_v = 0.8, \Omega_{\rm CDM} = 0.2, {\rm h} = 0.8$; Dash-dot line : C + HDM model with $\Omega_{\rm CDM} = 0.7, \Omega_{\rm HDM} = 0.3$; Dotted line : CDM model with $b = 2.5$

Fig. 2: Non-linear evolution of the power spectrum based on N-body simulations.

Fig. 3: (a) (Top) A slice of the universe for a power spectrum $P(k) \propto k^{-1}$ in 2D. This is obtained by moving the particles in a potential which is frozen in time. (b) (Bottom) The corresponding slice of the universe obtained from exact N-body evolution. The similarity between (a) and (b) shows that the key feature of cosmological evolution is in moving the particles towards the minima of the potential.

Fig. 4: The contribution $\Omega(M)$ due to collapsed objects at different redshifts as a function of $\sigma(M)$. Since Abell clusters (at $z = 0$) contribute $\Omega \simeq (0.001 - 0.02)$ we need $\sigma(M) \simeq (0.5 - 0.7)$ at cluster scales. Similarly, since damped Lyman alpha systems contribute $\Omega \simeq (0.04 - 0.1)$ in the redshift range of $z \simeq (2 - 3)$ we need $\sigma(M) \simeq (2.5 - 4.1)$ at the mass scales of $M \simeq (10^{11} - 10^{12}) M_{\odot}$.

Fig. 5: Constraints on $\sigma(R)$ from different observations. See text for the discussion.

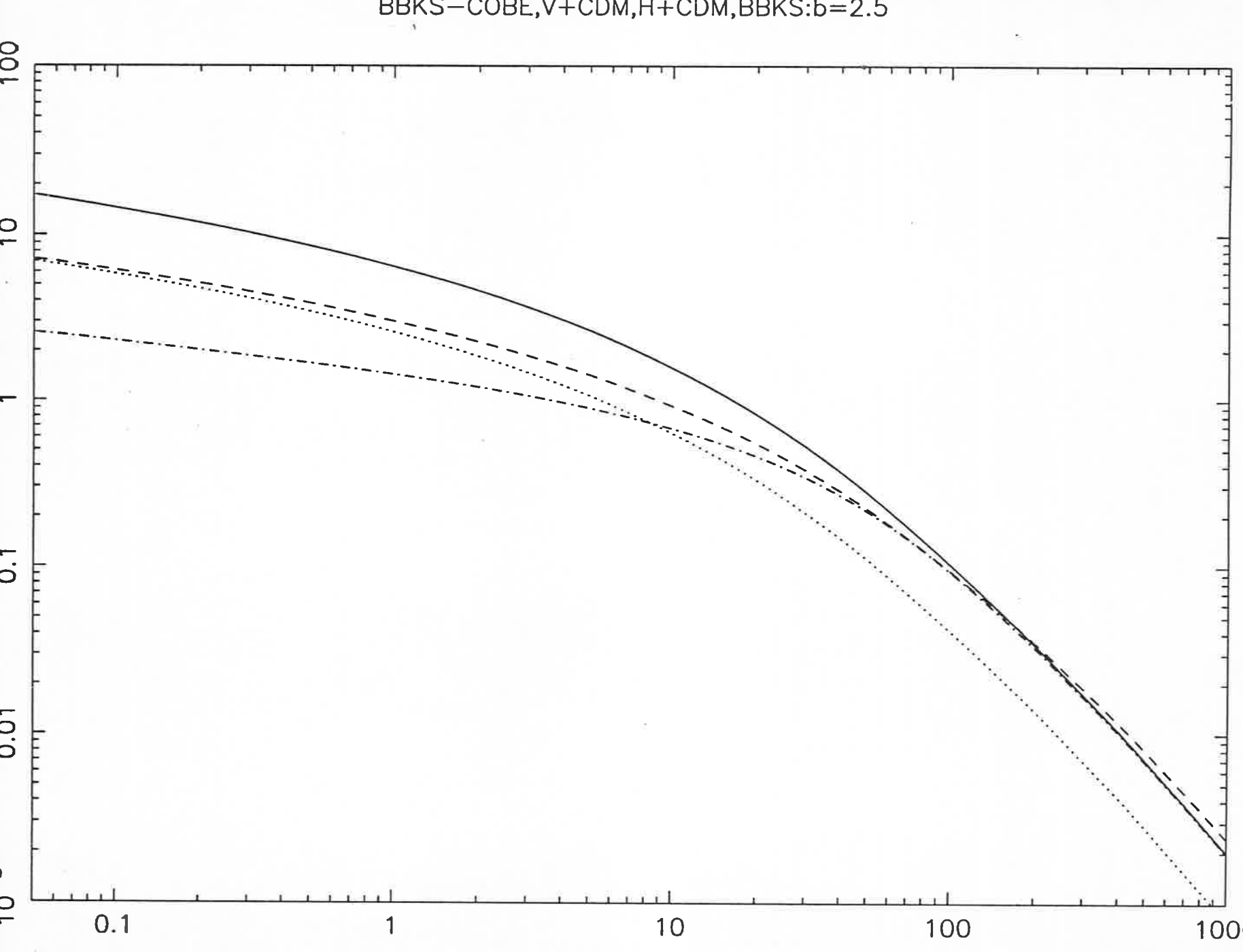

Fig. 1

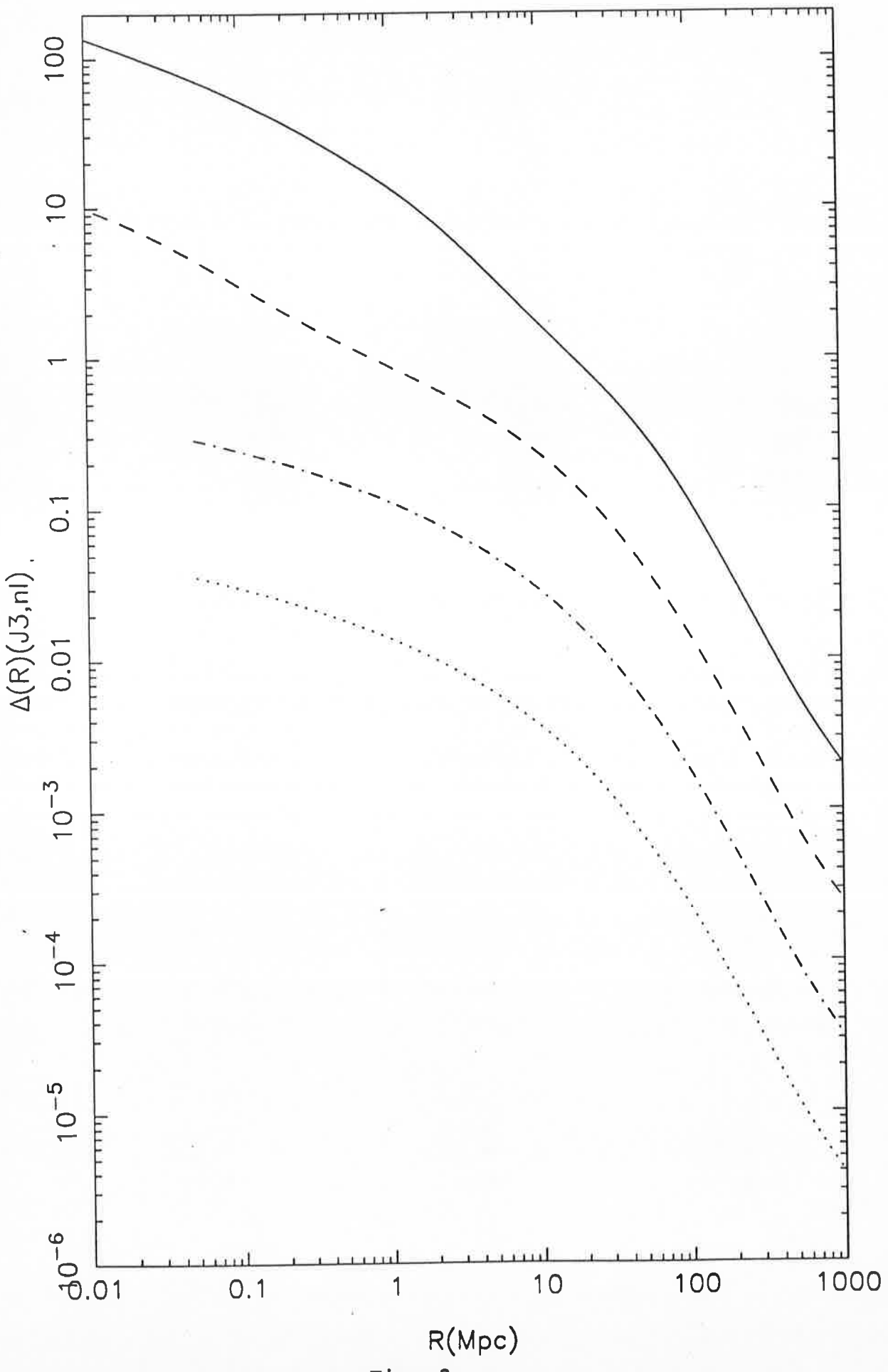
BBKS−COBE,z=0,7,63,511
Δ(R)(J3,nl)
R(Mpc)
100
10
1
0.1
0.01
10^-3
10^-4
10^-5
10^-6
0.01
0.1
1
10
100
1000

Fig. 2

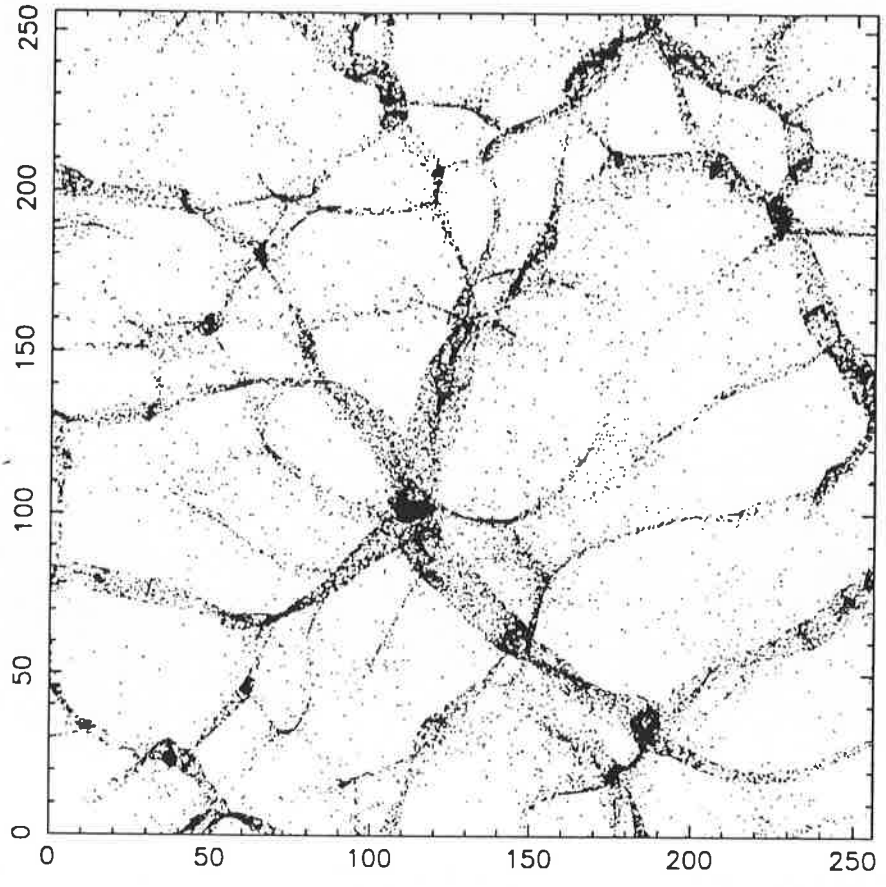

Fig. 3a

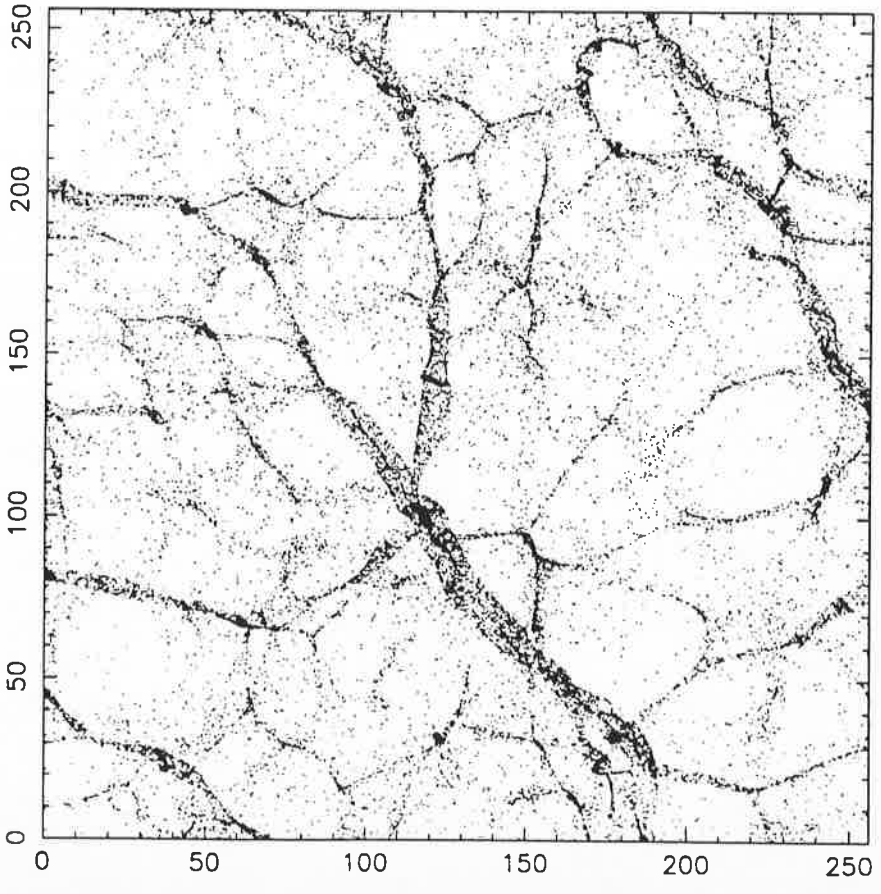

Fig. 3b

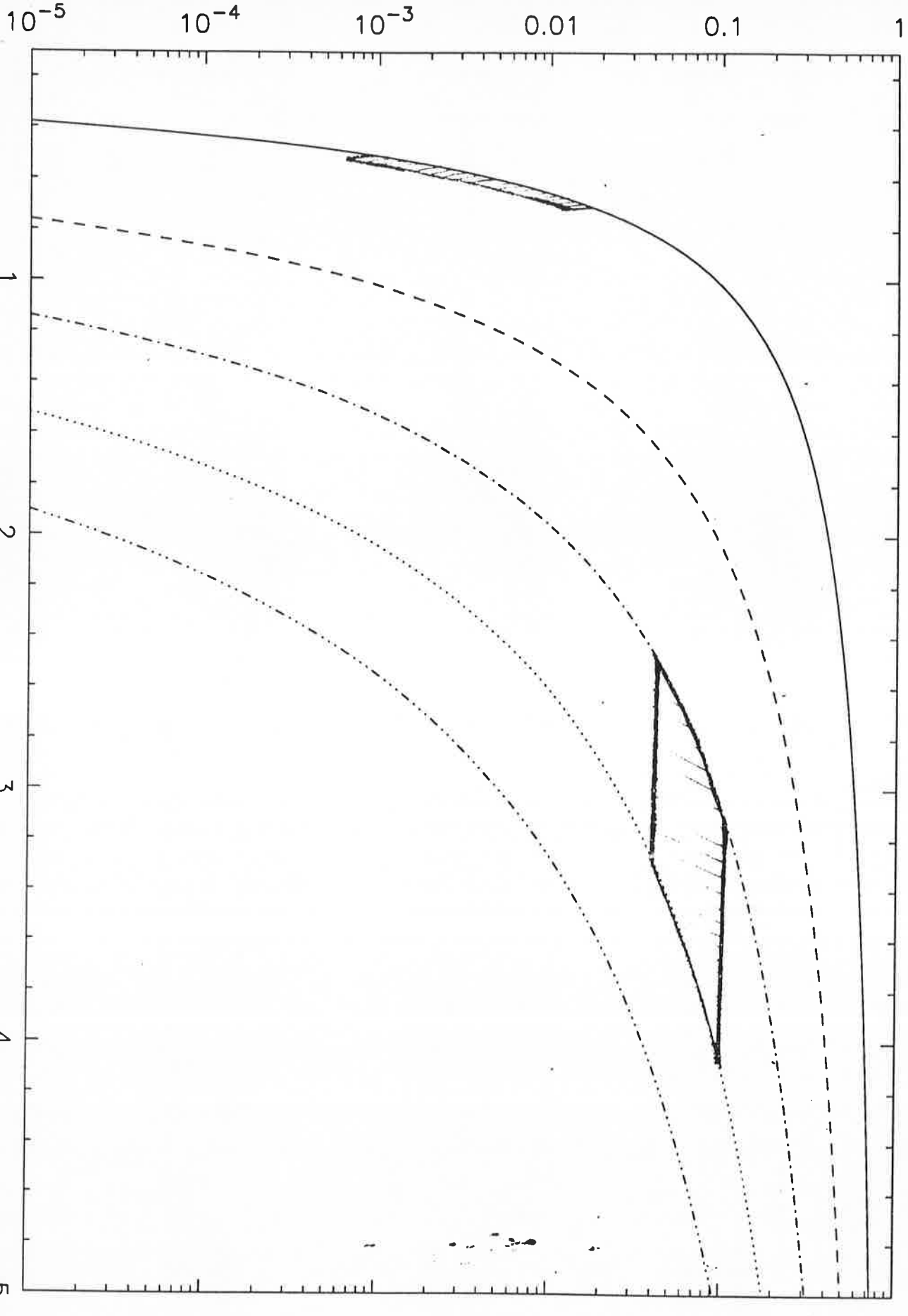

Fig. 4

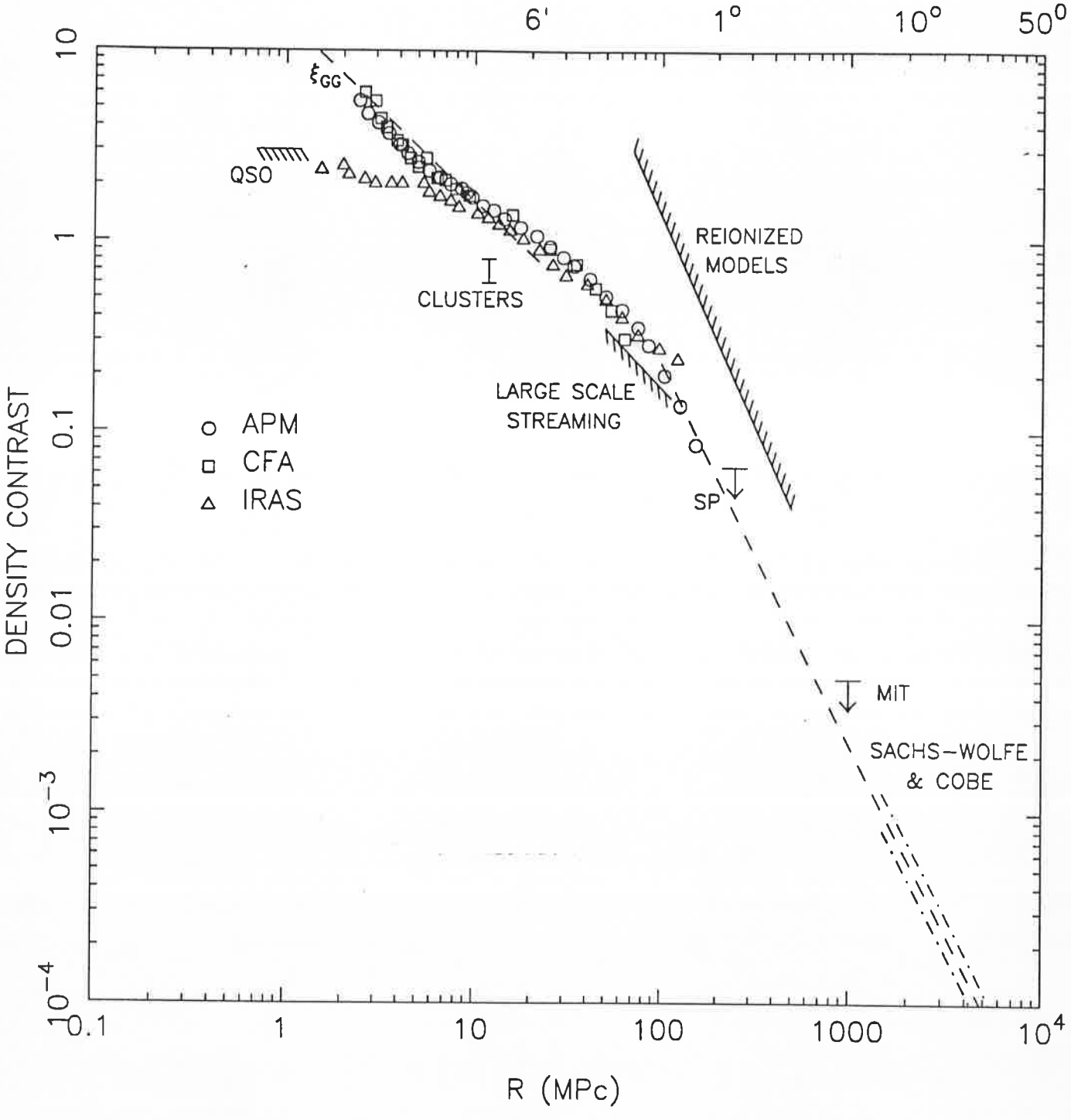
6'
1°
10°
50°
10
1
0.1
0.01
10^{-3}
10^{-4}
DENSITY CONTRAST
ξ_{GG}
QSO
CLUSTERS
REIONIZED
MODELS
LARGE SCALE
STREAMING
APM
CFA
IRAS
SP
MIT
SACHS–WOLFE
& COBE
0.1
1
10
100
1000
10^4
R (MPc)

Fig. 5